
ASSOCIATION: REMIND YOUR GAN NOT TO FORGET

Yi Gu[†] Yuting Gao[‡] Ruoxin Chen[†] Feiyang Cai[§] Jie Li[†] * Chentao Wu[†]
[†] Department of Computer Science and Engineering, Shanghai Jiao Tong University, Shanghai, China
[‡] Department of Electrical and Computer Engineering, Texas A&M University, College Station, US
[§] Department of Medicine, McGill University, Montreal, Canada
{louisgu, lijiecs}@sjtu.edu.cn

November 30, 2020

ABSTRACT

Neural networks are susceptible to catastrophic forgetting. They fail to preserve previously acquired knowledge when adapting to new tasks. Inspired by human associative memory system, we propose a brain-like approach that imitates the associative learning process to achieve continual learning. We design a heuristics mechanism to potentiatively stimulates the model, which guides the model to recall the historical episodes based on the current circumstance and obtained association experience. Besides, a distillation measure is added to depressively alter the efficacy of synaptic transmission, which dampens the feature reconstruction learning for new task. The framework is mediated by potentiation and depression stimulation that play opposing roles in directing synaptic and behavioral plasticity. It requires no access to the original data and is more similar to human cognitive process. Experiments demonstrate the effectiveness of our method in alleviating catastrophic forgetting on continual image reconstruction problems.

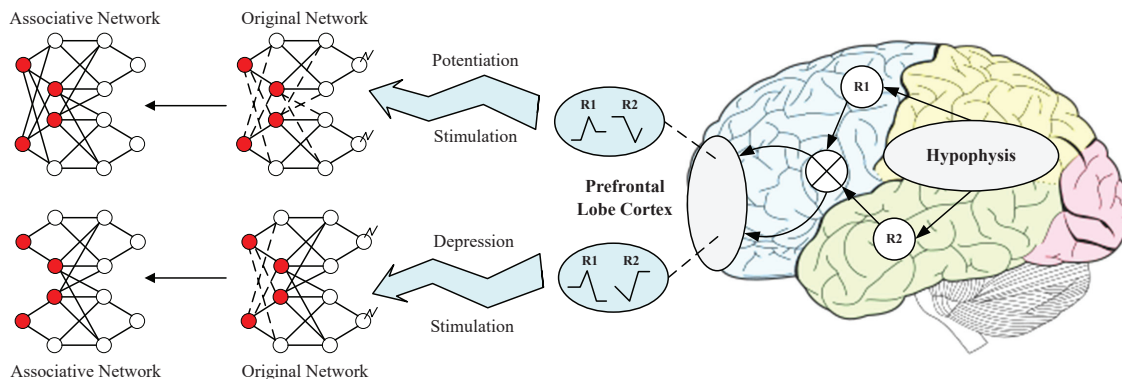


Figure 1: The formation of association depends on the dopaminergic reinforcement mediated by two dopamine receptors, DopR1 and DopR2. These two signaling cascades exhibit different temporal sensitivity, instructing opposing influences on associative learning.

1 Introduction

When tasks or datasets are sequentially and separately fed into the neural network for training, the model usually inevitably encounters the phenomenon of catastrophic forgetting [1]. The network constantly learns new training samples whilst forgetting the knowledge obtained from previous tasks. This results in an arbitrary degradation in the model performance on historical tasks. Continual learning or lifelong learning is still a long-standing open problem.

Although some efforts [2, 3, 4] have been devoted to tackle the catastrophe forgetting of discriminative models, image generation models, like most image classification ones, still consider that all data is available. It remains an under-explored area for generative models to acquire the continual learning capability, especially for paired image translation task. Different from the discriminative task, the continual learning for paired image translation task has intrinsic characteristics. Each training input for the discriminative model has a fixed corresponding label and the output is discrete. However, the generative model output is coherent, which requires the model to maintain the visual perception, i.e., the prediction should be semantically plausible and visually satisfactory. Therefore, the continual learning for paired image generation task can be formulated as enabling the neural network to perceive the reconstruction to new domains while memorizing captured representations.

Memory replay [5, 6, 7] is a common approach to solve catastrophic forgetting. It usually saves original images or extracted features of historical tasks, and revisit them when the network trains new task. However, this approach requires additional storage, and human learning knowledge is not like this mode of mechanically remembering data in essence. We are learning new knowledge every day and learning is a lifelong process. In fact, human tend to incorporate the acquired experience and summarize the correlation between two successively happening events. For example, when we see a fishing rod, we may think of fish. This memory and cognition mechanism is association.

Human leverage connections between relative things to associate new memory with recalled past memories, which makes the new knowledge learning more efficient and versatile. The ability of associative learning is critically determined by neuron network in association cortex. When human brain receives a stimulus from a certain cortex, the screen of events related to the stimulus will appear in the cortex. In the associative learning mode, some neurons are repeatedly stimulated, altering the efficacy of the synaptic transmission. We call this phenomenon synaptic plasticity, which facilitates or represses synaptic transmission by regulating the postsynaptic potential (PSP). If the stimulation is long enough, such PSP will have long-term alteration, including potentiation and depression [8]. Hence, a sensory stimulation will activate relative neurons, and other irresponsible neurons will be activated by these neurons, which leads to association.

Motivated by this biological mechanism, we propose to imitate the human associative learning to achieve the continual learning for image generation. We design a heuristics module to produce potentiation stimulations for the generative model. Once the signal is released to the model, it triggers synaptic plasticity to alter the efficacy of synaptic transmission, which associate the current screen with historical representation. However, the heuristics module only observes the single side of reconstruction to past domains. Similar to the depression influence in the brain, we also utilize a distillation approach to distill past knowledge to new domains. This approach takes inspiration from regularization countermeasures [9, 10, 11] characterized by adding extra constraints to consolidate acquired knowledge. Note that since we do not preserve raw data, we adopt the feature distillation to adapt the associated feature representation to the updated feature space. Our brain-like associative learning model, Assoc-GAN, does not require access to data of old tasks, and is closer to the nature of human learning and cognition.

Contributions in this paper include: (1) We simulate the human associative learning process and propose a brain-like continual learning framework for the generative model. (2) We design a heuristics module to heuristically associate the current scene with the historical representation, which does not require memorizing data and is more in line with the cognitive neuroscience of human memory. (3) We verify the significance of our method in alleviating catastrophic forgetting for challenging image reconstruction tasks.

2 Related Work

2.1 Associative Learning

Associative learning is classified into classical conditioning and operant conditioning. Classical conditioning refers to learning associations between a pair of stimulations, while operant conditioning refers to learning between behaviors and consequences [12]. Associative learning forms non-declarative memory or implicit memory, which is developed unconsciously and is independent of medial temporal lobe and hippocampus [13].

A reputed model is introduced to explain associative learning [14]. In the model, association cortex network is composed of millions of neurons, each of which can receive input spikes from thousands of other neurons. The distributed region of the association cortex is a set of brain regions that comprises extensive portions of the frontal and posterior midline and inferior parietal lobule [15]. Prefrontal cortex is the top-level of association cortex. It regulates associative learning and divergent thinking, which contributes to the abstract reasoning ability. Word fluency test, which requires examinees to write words beginning with certain letter, is used to quantify the capability of association. A study shows that prefrontal cortex damage impaired association [16]. Thus, association cortex, especially prefrontal cortex, enables associative learning.

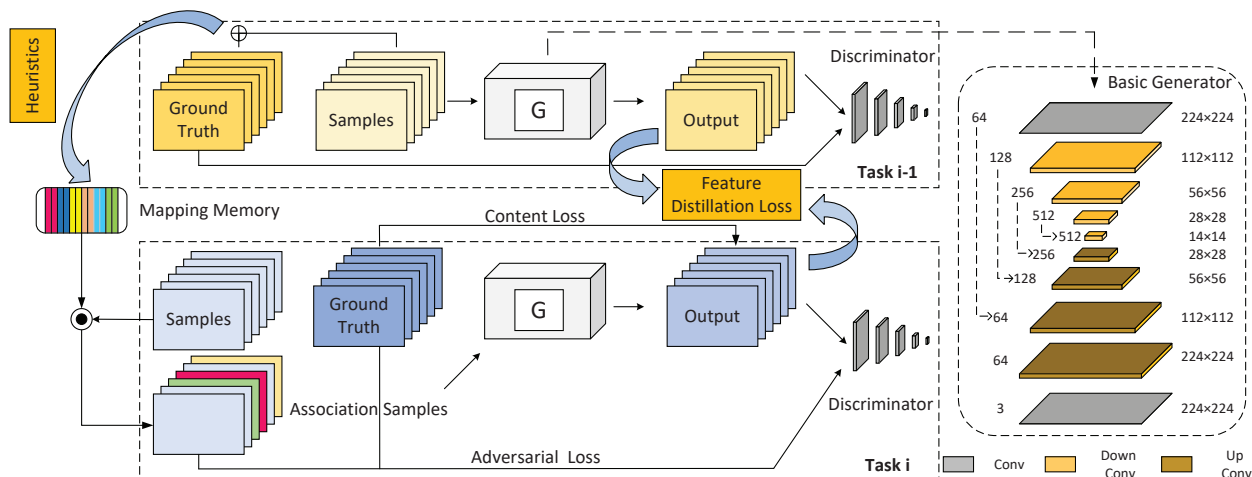


Figure 2: Overview of Assoc-GAN. For task i , the model learns to adapt to new environment using given current training samples. To handle the catastrophic forgetting, a heuristics module is adopted to potentially associate the current domain with the historical one, and a feature distillation is added to depressively slow down the update of knowledge to the new feature space.

Recently, many studies try to reveal the function of specific neuron and molecule in association cortex network. Typically, Cho et al. [17] find that γ -frequency synchrony between prefrontal parvalbumin interneurons is indispensable in associative learning. Handler et al. [18] reveal that dopamine-receptor signaling flexibly modulates the associations in a dynamic environment. Moreover, Mukherjee et al. [19] show that prelimbic and infralimbic cortex connectivity is essential for associative learning. However, restricted by imaging techniques, researchers cannot restore the distribution of every neuron or analyze the association cortex network precisely, but they find some features of the network as presented above.

2.2 Continual Learning

In order to mitigate the catastrophic forgetting, some continual learning approaches are proposed and they can be summarized into three categories: dynamic architecture, regularization, and memory replay.

Dynamic architecture assigns individual sub-networks for different tasks. Progressive neural network [20] freezes previous networks and grow new ones. The lateral connections transfer information across the task. Dynamically Expandable Network (DEN) [21] performs selective retraining and dynamically assigns the capacity by adding new neurons. Motivated by Growing When Required (GWR) [22], [23] proposes a set of prediction-driven hierarchical self-organizing neural networks. In [24], Deep Generative Memory (DGM) depends on GAN with two masks for network weights (DGMw) and layer activations (DGMa), respectively. It also uses a dynamic network expansion mechanism to ensure sufficient capacity for new tasks.

Regularization often adds constraint to loss function, which keep the balance between remembering old tasks and learning new tasks. In learning without forgetting (LwF) [25], predictions of previous learned network and the current network are encouraged to be similar by the means of knowledge distillation [26]. Elastic weight consolidation (EWC) [27] preserves the information of previous task in a posterior measured by the diagonal of the Fisher information matrix. Motivated by EWC, incremental moment matching (IMM) [28] introduces the mean and mode method to merge the parameters from old and new tasks. Intelligent synapses (IS) [29] estimates weights online compared to EWC computes offline. [30] introduces a method to specify the catastrophic forgetting of each parameter in the neural network. [4] computes the upper bound of absolute forgetting which have a higher variance.

Memory replay usually stores some samples from historical tasks. Incremental classifier and representation learning (iCaRL) [31] learns a nearest-mean-of-exemplars classifier and feature vector simultaneously. Gradient Episodic Memory (GEM) [32] episodic memory to maintain a subset of learned task. Memory Replay GANs (MeRGAN) [33] relies on joint training with replay alignment for pure unpaired image generation. Representation in [7] consists of the pseudo-sample from old task produced by generator and new sample, and it proves effective in the classification task. [3] is mask-based method and each layer dynamically generate mask given the input.

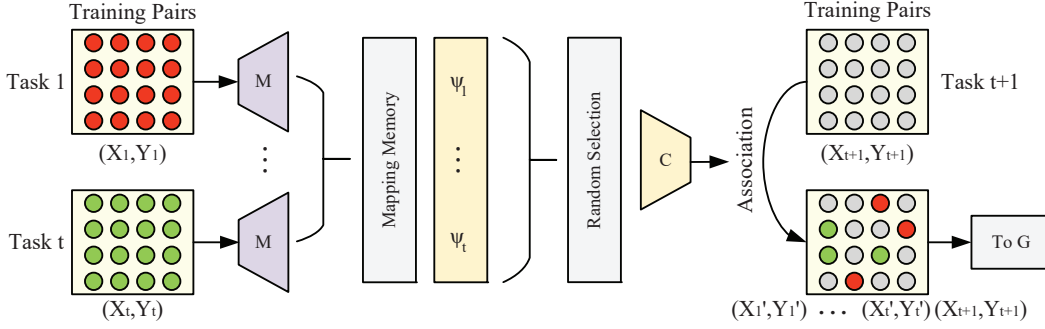


Figure 3: Heuristics module captures domain mappings from training pairs of each task and stores them into a memory structure. Then it applies the inverse mappings from the memory to reconstruct tensors and remaps them to the previous task domains. The association features will participate in the basic generator training along with the original features.

2.3 Paired Image Translation

Image generation has achieved great success since the advances of GANs [34]. This work has been applied in numerous fields like image inpainting [35], image completion [36], image reconstruction [37] and image restoration [38]. Recently GANs have made great progress in respect of paired image translation, which can be divided into two categories. The first method focuses on the unsupervised setting, which employs the unpaired data from different domains to establish the cross-domain mapping [39, 40, 41]. The second method follows the supervised setting, which seeks the reconstruction mapping between the input image and target image in a pixel by pixel manner [42, 43, 44]. To the best of our knowledge, we are the first to explore the continual learning for paired image translation, which requires the model to produce visually photo-realistic images among all tasks while only rely on the training of current paired samples.

3 Brain-inspired Associative Learning

3.1 Preliminary

Generative network aims to learn a non-linear transformation from source space to target space, which requires pixel-wise supervision. We follow the architectural guidelines of U-Net [45] as basic generator, which proves the efficacy and simplicity in the pixel-wise prediction of the semantic segmentation, as shown in Figure 2. Note that we modify the padding scheme of each convolution layer to keep the input image and output image the same size. To ensure that the prediction is visually realistic and perceptually coherent, we use the discriminative network to distinguish generated images from original ones. Here, the architecture of discriminator is the same as [46] to maintain the generated content to be consistent with the surrounding contexts.

Training is an adversarial process introduced by [34], where the generator G competes with the discriminator D and the two networks are optimized alternately. G aims to generate content that can deceive D while the goal of D is to distinguish between generated samples and real ones. The game can be defined as a minimax objective function:

$$\max_{\theta_D} \min_{\theta_G} \mathbb{E}_{z \sim \mathbb{P}_g} [1 - \log(D(G(z; \theta_G); \theta_D))] + \mathbb{E}_{\tilde{z} \sim \mathbb{P}_d} [\log(D(\tilde{z}; \theta_D))]. \quad (1)$$

where θ_D denotes the parameter of D , θ_G denotes the parameter of G , \tilde{z} is the target sample subjecting to the real data distribution \mathbb{P}_d while z is the source sample subjecting to the mimicked data distribution \mathbb{P}_g . We adopt the content and adversarial loss from some GAN approaches [47] [42] to optimize the generator network.

Content loss. Pixel-wise L2 or MSE loss is a classic choice for measuring the perceptual similarity between generated images and original ones. This loss enforces the output produced by the generator to be close to the ground truth, further bridging the input-output gap, formulated as:

$$\mathcal{L}_{mse} = \frac{1}{CWH} \sum_{i=1}^N \left\| \tilde{z}^{(i)} - G_{\theta_G}(z^{(i)}) \right\|_2, \quad (2)$$

where $G_{\theta_G}(z^{(i)})$ is the generated image and C, W, H correspond to the channel, weight and height of the image.

Adversarial loss. It is adopted to encourage the generator to produce the natural-looking images that manage to fool the discriminator, formulated as:

$$\mathcal{L}_{adv} = \sum_{i=1}^N -\log D_{\theta_D}(G_{\theta_G}(z^{(i)})), \quad (3)$$

where $D_{\theta_D}(G_{\theta_G}(z^{(i)}))$ represents the probability of the discriminator over the prediction.

Therefore, we use content loss to produce general content and adversarial loss to complete texture details. The overall loss function can be formulated as:

$$\mathcal{L} = \mathcal{L}_{mse} + \lambda \mathcal{L}_{adv}. \quad (4)$$

where λ is the trade-off weight, which is set by the cross-validation experiments.

3.2 Heuristics Module

We suppose a sequence of N tasks to be learned in order, $T = \{T_1, \dots, T_N\}$. Each task T_i is given a dataset of N_i paired instances, $T_i = \{\mathcal{X}_{i,j}, \mathcal{Y}_{i,j}\}_{j=1}^{N_i}$, where \mathcal{X}_i and \mathcal{Y}_i denote the original domain and ground truth domain respectively. In training session, the i -th model H_i learns the current task T_i and aims to optimize the neural network to replicate T_i 's real data distribution \mathbb{P}_i . Besides, H_i should also maintain the ability to generate competitive results on the previous tasks T_1, \dots, T_{i-1} . However, the model has no access to the previous training data and can only use current data $\{\mathcal{X}_i, \mathcal{Y}_i\}$. Unlike previous efforts mainly designed for image classifiers, image generation is typically more challenging than classification.

As discussed in Section 1, human can heuristically associate one picture with another relative picture. This is due to the nature of neuroscience that the formation and update of association are mediated by potentiation and depression stimulation. As shown in the associative learning model in Figure 1, every node represents a neuron, and red nodes refer to neurons that are essential for associative learning. Normally, primitive and stable connections exist between neurons, which are represented by full lines. If two dopamine receptors, DopR1 and DopR2, stimulate almost at the same time and repeatedly in the network, the original network will be trained into an associative network [18]. To be more specific, backward pairing of DopR1 and DopR2 ensures the potentiation, and weak connections between neurons, which are represented by dotted lines, will be potentiated to stable connections. Otherwise, the forward pairing of DopR1 and DopR2 induces the depression, and weak connections will be depressed to cut off connections.

Motivated by this mechanism, the target model can also be formulated as the interaction of potentiatively guiding the association of past knowledge and depressively allowing the learning of new episodes. We propose to preserve the initial mapping between target and source domains which captures concepts when encountering new domains. This is similar to potentiation mechanism that reconstruct connections between stimulated neurons and associative neurons.

Fig 3 illustrates the heuristics module applied to our framework. First, when the basic generator is trained for the $i-1$ -th task T_{i-1} , a mapping agent M learns to memorize the cumulative input space and record the reconstruction mapping, $\psi_{i-1} : \mathcal{X}_{i-1} \rightarrow \mathcal{Y}_{i-1}$. Then, for the i -th task, the generator obtain new training paired samples $\{\mathcal{X}_i, \mathcal{Y}_i\}$. A controller C randomly selects mappings from the mapping memory to perform inverse mapping which reconstructs the current input space, $\psi_i^{-1} : \mathcal{Y}_i \rightarrow \{\mathcal{X}_j\}_{j=1}^{i-1}$. It associates part of current ground truth with the training samples of previous tasks, which avoid saving original images or extracted features. Moreover, the data distribution \mathbb{P}_i will itself experience gradual generalization of concepts to new domains without forgetting the past distribution \mathbb{P}_{past} at any moment. In other words, the generative model is continuously capturing and updating knowledge about past domains. Therefore, the objective function of the i -th task can be formulated as

$$\begin{aligned} \min_{\theta_i} \{ & (1-r) \mathbb{E}_{\{\mathcal{X}_i, \mathcal{Y}_i\} \sim \mathbb{P}_i} [\mathcal{L}(G^i(\mathcal{X}_i; \theta_i), \mathcal{Y}_i)] \\ & + r \mathbb{E}_{\{\mathcal{X}'_i, \mathcal{Y}_i\} \sim \mathbb{P}_{past}} [\mathcal{L}(G^i(\psi^{-1}(\mathcal{Y}_i; \theta_i)), \mathcal{Y}_i)] \}. \end{aligned} \quad (5)$$

where θ_i are parameters of the i -th generator network and r is the association ratio at the current task training data.

The proposed module can employ any deep network architecture, and we utilize the network where the architecture is the same as [39] to obtain memorized mappings for association selection.

3.3 Feature Distillation Loss

The heuristics module is only updated along the single side trajectory from \mathbb{P}_i to \mathbb{P}_{past} during the i -th task training process. Inspired by [25] which adopts regularization term to maintain the performance of discriminative models

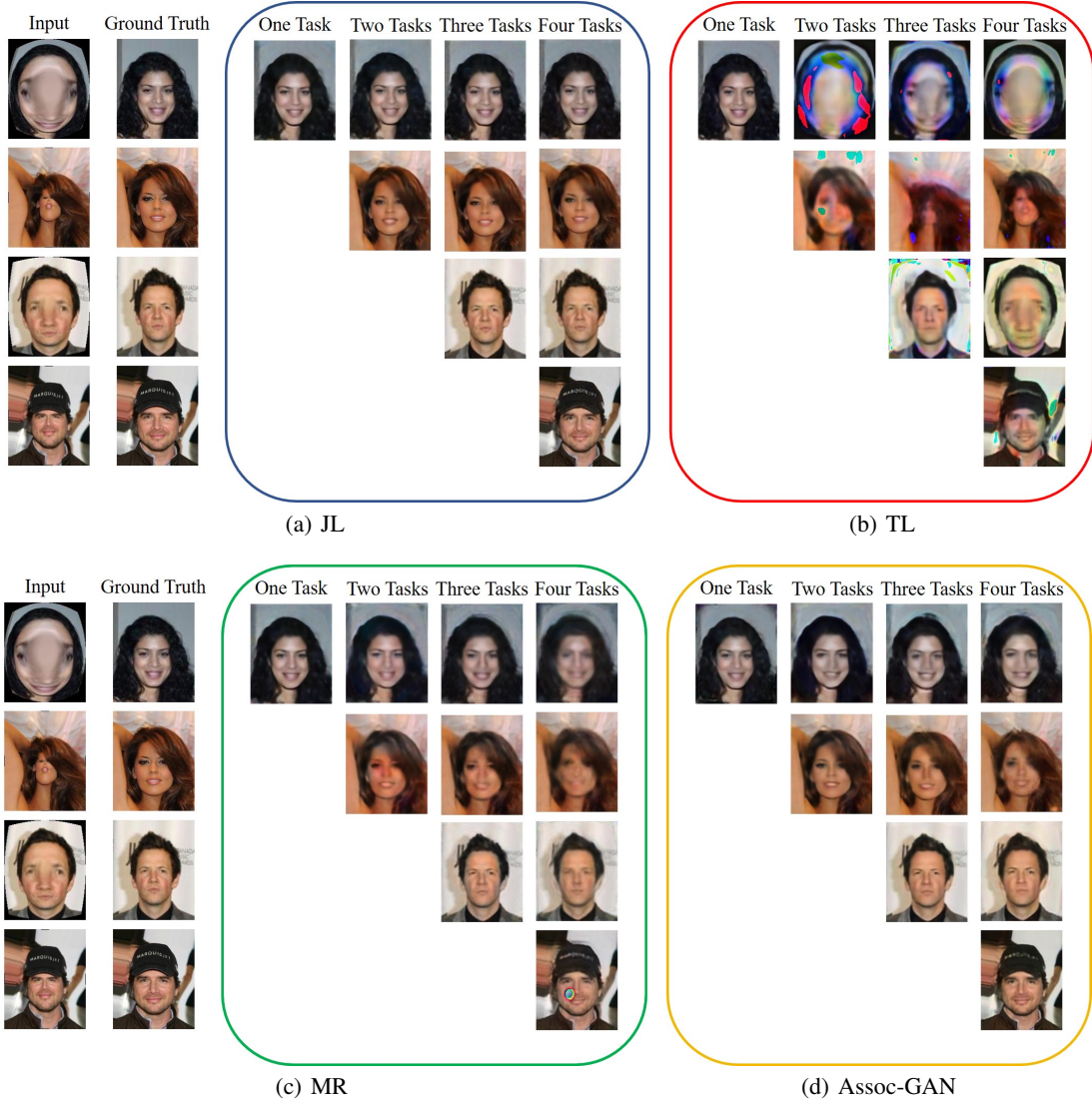


Figure 4: Comparison among different methods for continual learning of image reconstruction tasks.

on previous tasks, we utilize the knowledge distillation to perform depression in the generative network. This term is similar to human depression mechanism that the plasticity of synapses is reduced to alter the efficacy of synaptic transmission. Our distillation loss aims to reduce the empirical risk between current samples and past ones, while the historical knowledge is more effectively retained by heuristics memory system as discussed in Section 3.2.

Specifically, after task T_{i-1} is trained, the parameters θ_{i-1} of model G^{i-1} will be saved as the existing knowledge for the next task T_i . We feed the current training samples $\{\mathcal{X}_i, \mathcal{Y}_i\}$ into G^{i-1} and G^i and distill the knowledge to restrict the parameters, which weakly inhibits the target model adaption to the new task and encourage G^i to produce similar outputs to G^{i-1} . We adopt the cosine normalization [48] where the prediction is based on cosine similarity instead of dot product in neural networks. It transfers feature knowledge between feature spaces of different tasks, alleviating over drifting in feature domains. [49] has demonstrated the effectiveness of cosine normalization applied to the image feature vectors, which replaces the standard knowledge distillation loss [26] and improves the accuracy of discriminative model.

Therefore, the optimization problem on feature distillation can be defined as the transfer of knowledge from past distribution \mathbb{P}_{past} to refined distribution \mathbb{P}_i for approximation by minimizing the cosine distance:

$$\mathcal{L}_{feature} = 1 - \cos \langle G^i(x_i; \theta_i), G^{i-1}(x_i; \theta_i) \rangle, \quad (6)$$

where the former term and the latter one are prediction results generated by G^i and G^{i-1} at task step i , respectively.

		SSIM				PSNR			
		One task	Two tasks	Three tasks	Four tasks	One task	Two tasks	Three tasks	Four tasks
JL	Task1	0.86	0.82	0.83	0.81	29.65	27.85	28.36	26.59
	Task2		0.83	0.83	0.83		26.92	27.22	26.52
	Task3			0.89	0.88			31.23	28.51
	Task4				0.91				30.31
	average	0.86	0.83	0.85	0.86	29.65	27.39	28.94	27.98
TL	Task1	0.81	0.30	0.37	0.29	27.02	9.73	12.07	9.87
	Task2		0.74	0.47	0.51		23.23	13.34	14.94
	Task3			0.80	0.37			26.28	11.86
	Task4				0.85				27.06
	average	0.81	0.52	0.55	0.51	27.02	16.48	17.23	15.93
MR	Task1	0.78	0.69	0.71	0.68	26.20	22.74	23.54	23.12
	Task2		0.74	0.74	0.71		22.74	23.31	20.19
	Task3			0.82	0.78			26.62	25.23
	Task4				0.84				23.44
	average	0.78	0.72	0.76	0.75	26.20	22.74	24.49	23.00
Assoc-GAN	Task1	0.75	0.69	0.65	0.63	23.32	22.03	20.31	20.11
	Task2		0.77	0.72	0.61		24.56	22.28	18.95
	Task3			0.82	0.75			27.23	24.40
	Task4				0.83				27.55
	average	0.75	0.73	0.73	0.71	23.32	23.30	23.27	22.75

Table 1: Quantitative evaluations in terms of PSNR and SSIM. Higher values are better.

The feature distillation loss guides the parameters of current circumstance θ_i to be similar to those shared by past task θ_{i-1} , and this regularization term is an additional distillation for feature rather than logits. It only depends on the previous task parameters θ_{i-1} without additional storage throughout the whole training process.

We combine the feature distillation loss with the basic loss, and the new loss function of our framework can be formulated as:

$$\mathcal{L}' = \mathcal{L}_{mse} + \lambda_1 \mathcal{L}_{adv} + \lambda_2 \mathcal{L}_{feature}. \quad (7)$$

where λ_1, λ_2 are the new trade-off weights.

The modified loss function enforces the model to update parameters to reconstruct the old experience as well as the new one. It preserves relevant past experience and generalize the concept to new domains. Therefore, the model can still continually retain the distribution of past domains \mathbb{P}_{past} while integrating new tasks.

4 Experiment

4.1 Implement Details

We explore the continual learning for paired image translation through qualitative and quantitative analysis. The qualitative evaluation mainly relies on visual perception while the quantitative evaluation utilizes peak signal to noise ratio (PSNR) and structural similarity (SSIM) to quantify the performance. We estimate our method on distorted face dataset (DFD) [50], which is a challenging reconstruction task for distorted face restoration. We split the DFD into four tasks according to distortion types and degrees. All images for training and testing are size of 224×224 . We initialize the trade-off weight λ_1 as 0.001, λ_2 as 0.2 and the learning rate as 0.01. All experiments are conducted on Tesla V100.

4.2 Baseline Models

To the best of our knowledge, this domain is still considering that all training samples are available and there is no continual learning method reporting results. We design the following baseline methods and compare our model with them: (a) Joint Learning (JL). Data of all tasks is learned together. This is the theoretical upper bound of continual learning. (b) Transfer Learning (TL). The data of each task is fed into the model sequentially for training. We use the parameters obtained from the previous task to initialize the current task model, so that preserved knowledge can be fully leveraged. (c) Memory Replay (MR). We randomly select samples of previous tasks and store them in raw format. When the model learns new episodes, previous tasks samples will be replayed.

4.3 Qualitative Results

Reconstruction generation results are summarized in Figure 4. These results illustrate that our inference model obtains predictions indistinguishable from ground truth and works well on split DFD. We also compare Assoc-GAN with other three models. The results show that JL performs better than other methods and achieves the most visually satisfactory results, which is the upper bound of continual learning. The results of MR are visually close to those of Assoc-GAN, indicating that both can effectively deal with catastrophic forgetting. But historical outputs of MR seem increasingly blurry and some reinforced generation artifacts [51] exist. The reason is that MR is more sensitive to artifacts and will be reinforced during intermediate task training [10], while Assoc-GAN shows more robustness and less sensitiveness to them. TL is unable to capture previous concepts and suffers from catastrophic forgetting. Note that the greater distortion degree, the more details lost in the produced results, so tasks 1 and 2 themselves are more difficult to restore than tasks 3 and 4. Overall, the hallucinated results produced by Assoc-GAN are perceptually convincing and it performs particularly well on all four tasks without forgetting historical knowledge.

4.4 Quantitative Results

Table 1 presents the SSIM and PSNR results for quantitative evaluation. JL is not subject to continual learning conditions, and it takes the achievement of the highest numerical performance for granted, which sets up the upper bound for continual learning. TL only generates incoherent facade-like patterns and obviously completely forgets the acquired knowledge. Assoc-GAN has no access to original images and obtains promising results in comparison to MR, while the latter directly revisits past training data. It also retains the content coherence and does not to be influenced by changing circumstances. We can conclude that Assoc-GAN illustrates good generalization ability on all four tasks, due to the nature of our method, which can potentiate the avoidance by heuristics module and depress the attraction the by feature distillation loss. Note that as the distortion degree increases, both the two metrics decreases.

4.5 Memory

As shown in Figure 5(a), we estimate the viability of Assoc-GAN usage in the term of memory requirement. In addition to the current task data, MR and JL also need extra memory to store the previous task data. It can be observed that as task number increase, the memory overhead of MR and JL shows a non-linear increase, while Assoc-GAN increases almost linearly, and the memory usage is much lower than the previous two methods. In the case of training four tasks, when PSNR of each model reaches an almost all equal state, our memory overhead is only 20.9% of MR and 5.9% of JL, respectively. Consistently we can claim that Assoc-GAN is suitable for deployment and occupied storage size does not increase significantly compared with MR and JL.

4.6 Quota

Figure 5(b) illustrates the average PSNR along the sequential training, during which new tasks are transited to the model. JL is the upper bound. TL consistently achieves competitive results on the latest task while forgetting most previous tasks. The discrepancy between MR and Assoc-GAN is relatively small, and Assoc-GAN can quantitatively obtains comparable performance to MR. However, since MR and JL directly revisits original training samples, the perceptual quality of predictions may degrade when totally different task with inverse data distribution gradually participate in the training. The update of knowledge continually interferes with retained knowledge, and the imbalance between new and old task samples incur more fluctuations. The amplitude of JL is 2.26 dB and that of MR is 5.04 dB, but ours is only 0.57 dB. This is because feature distillation loss intermediate the stability and plasticity, which slows down the performance decay on all incremental steps. It demonstrates that other methods are more sensitive to the quota compared with Assoc-GAN while our method can effectively reduce this bias and maintain the robustness of performance.

4.7 Sequence

Figure 5(c) demonstrates the effect of task arrival sequence on final performance and we can derive some findings on the tasks exposed to the model. In general, the more recent the task, the better the model performance. However, the performance does not systematically reduce all the time. Except for TL, PSNR of other three methods on task 2 is lower than that of task 1. MR drops by 12.7% while Assoc-GAN drops by 5.8%. In fact, task 2 and task 1 belong to different distortion types. It indicates that when new samples are totally different from what has been presented before, some new knowledge should be learned from new training samples. When they are fed into the model, the model has to adapt to the new environment and minimize the interference of previous learning, so the performance may decrease. Conversely, if new samples are similar to the previous task domain, perceptually similar distortion types or degrees will

appear more frequently across different increment batches. With the assistance of knowledge accumulated by feature distillation loss, the performance of model may be improved again. For instance, PSNR of three methods on task3 all increase compared with task 2. In fact, task3 has similar distortion type with task1 but with different degree, the acquired knowledge is transferred to the training of task 3 in the form of distillation. TL does not have the ability to retain knowledge, so this law is unrepresentative to this type of method.

4.8 Forgetting

We observe the evolution of PSNR on task1 and task2 during the whole training process from Figure 5(d). Since JL trains all task data together each time, it achieves the best results. But it is easily to suffer from catastrophic forgetting. Once the task is separately input, the model will inevitably forget the historical knowledge like TL. In contrast to other methods, our model retains the previous task knowledge throughout sequential training on all cases. Both MR and Assoc-GAN generate competitive predictions but the knowledge forgetting speed under Assoc-GAN is slower than MR. It highlights the merits of our associative learning, i.e., continually updating knowledge by heuristic algorithm and generating results close to MR without using original data. It also reveals that Assoc-GAN even achieves a better performance than MR under some circumstances, which is attributed to the transferred knowledge within parameters of previous model. Adding heuristics module and feature distillation significantly mitigate the catastrophic forgetting and improve the performance in all cases, especially with incremental steps over long time range.

4.9 Training Time

Training time of each method is summarized in Figure 5 (g). The task size of each method remains consistent during training process. Note that since the time complexity of TL algorithm is the same as JL, we omit the TL and only list the training time of JL. JL combines all task data for training, so its training time increases as the number of tasks increases. The increased time of JL is related to the scale of task training samples, and the compound growth rate of JL in DFD tasks is 63.51%. MR only retains part of previous data, although the training time will also increase with the expansion of task scale, the time increase is not as much as JL. The compound growth rate of MR is 40.80%, which is 35.8% lower than JL.

Since our method has no access to original data or extracted feature, it utilizes the heuristics module to think of the previous circumstance from current training samples. During the training process, it only takes the time of heuristics module to backtrack the data, instead of training additional data. And regardless of the number of previous tasks, the time of our module’s backtracking is relatively fixed, only changing the occupancy ratio of each task in the total backtracking time. This makes the training time of our method irrelevant to the task size, which greatly reduces the growth rate of training time. The compound growth rate of our method is 7.87%, which is 87.6% and 80.7% lower than JL and MR, respectively. However, in each task training, our method needs to spend extra time extracting the mapping of domain conversion, so the training time of Assoc-GAN in a single task is longer than JL and MR. When training three tasks or less, the total training time of JL and MR are shorter than Assoc-GAN. But with the increase of task number, a turning point appears during training of four tasks, and the training time of JL and MR begin to surpass Assoc-GAN. Since the growth rates of these two methods are larger than that of Assoc-GAN, it can be foreseen that continually adding tasks to the model will make the computing power gap between these two methods and Assoc-GAN larger. We can conclude that Assoc-GAN is not cumbersome for training and the computing power overhead does not increase significantly compared with MR and JL.

4.10 Hyper Parameter

λ_2 is the only extra hyper parameter as shown in Eq. 7, which weights the balance between new and old knowledge. To understand the nature of this moderate update contributing to our solution, we adjust the λ_2 and observe the impact on model performance. Figure 5(e) and 5(f) show the impact on the average performance and the prior task performance, respectively. From Figure 5(e) we can find that these scattered points can be clustered into three categories, among which 0.4, 0.5, 0.6, and 0.7 are clustered into one category, and the performance of task 1 and 2 in this category are higher than other categories. Note that as the λ_2 increases, more of task performance is preserved, but at some point the PSNR decays. The point where PSNR of task 1 drops represents the optimum of the stability-plasticity curve. We also plot the final average PSNR for all the four tasks. As shown in Figure 5(f), the plateaus of PSNR indicates the balanced learning regime where the knowledge can be consolidated by updating the parameters, and λ_2 corresponding to it is 0.5. We identify the important hyper parameter to update knowledge where our model can confidently learn new tasks while still accumulating knowledge over time.

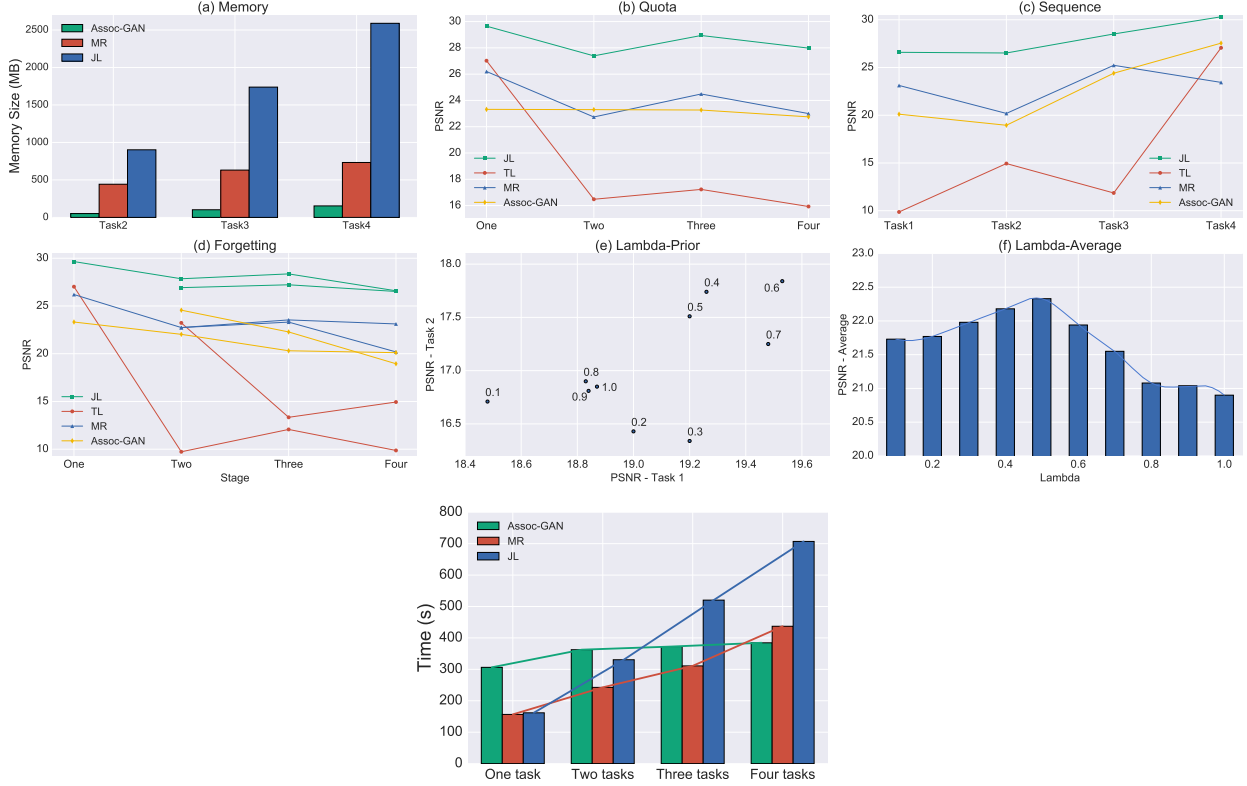


Figure 5: Performances on different methods for continual learning of image reconstruction tasks.

4.11 Ablation Study

We analyze each component of Assoc-GAN to illustrate each impact on model final performance. As shown in Table 2, UNet encounters complete failure and achieves the worst performance in all cases without the content loss. Moreover, the adversarial loss serves as an inpainting term for restoration, which is beneficial to capture the structure and encourages the network to produce sharp content. However, since tasks are reached sequentially and cannot be recurred in a long-time interval, it is necessary to utilize the heuristics module to reconstruct the current domain with large incremental steps. It illustrates that using the heuristics module improves PSNR from 14.03 dB to 22.09 dB and SSIM from 0.49 to 0.69, which contributes the most to the model performance. By adding distillation term, the two metrics are slightly improved and this is because it depresses the adaptation of new episode and guide the prediction coherent with previous circumstances. We can conclude that Assoc-GAN of exploiting feature distillation loss for the generative model proves beneficial. Ultimately, after all the components are added, our full model obtains the best results and a new state-of-art is established on this task for continual learning.

Module	PSNR	SSIM
UNet	6.13	0.05
UNet+ \mathcal{L}_{mse}	13.06	0.46
UNet+ \mathcal{L}_{mse} + \mathcal{L}_{adv}	14.03	0.49
UNet+ \mathcal{L}_{mse} + \mathcal{L}_{adv} +Heuristics	22.09	0.69
UNet+ \mathcal{L}_{mse} + \mathcal{L}_{adv} +Heuristics+ $\mathcal{L}_{feature}$	22.75	0.71

Table 2: Results of each module on four tasks training.

To verify the effectiveness of our proposed heuristics module for potentiative stimulation, we set the input and output of the heuristic module to three channels and only use the heuristic module to test Association capability on DFD. Our training process is still the same as before, and the model will save the mapping agent parameters after each task is trained. For one task, we adopt the inverse mappings of another three tasks for Associative generation. Figure 6 presents some examples of intermediate Association results on four tasks sequential training.

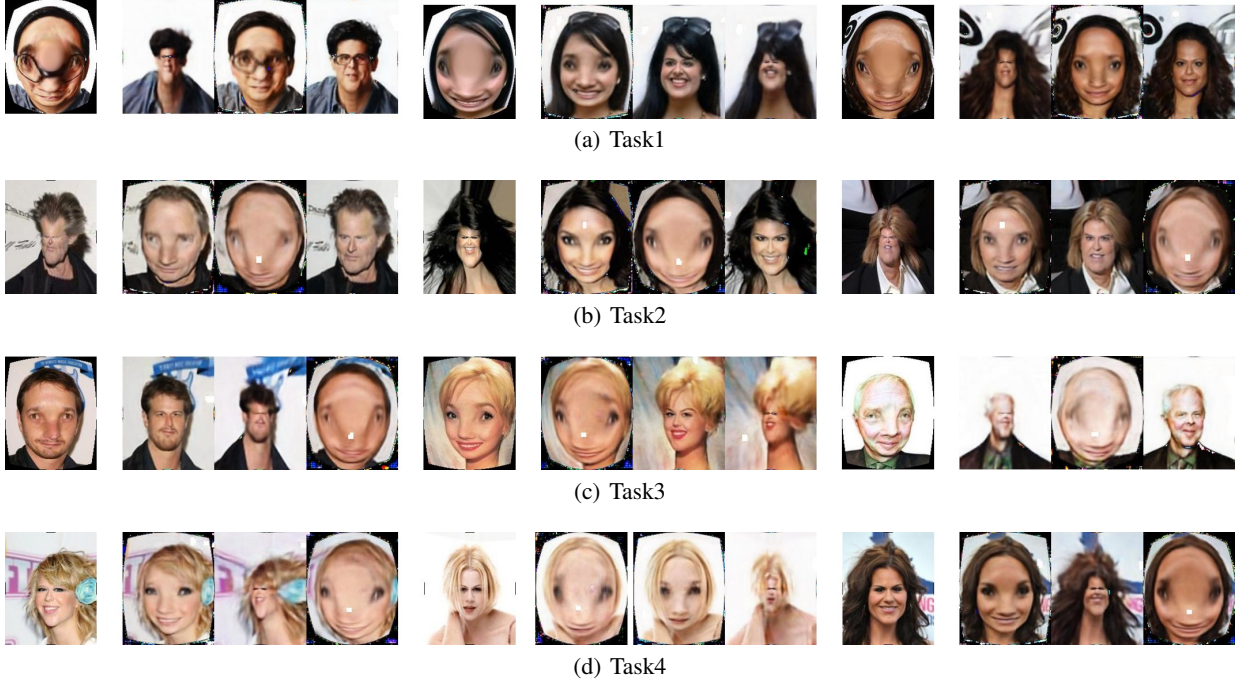


Figure 6: Some examples of Association image generated by our heuristics module. The first column of each group is the original distortion image, the second to fourth column are the Associative reconstruction image.

It can be seen that our heuristics module has learned different image transformations from one domain to another domain. The first column of each group in the figure is the distorted image of the current task, and the second to fourth columns are reconstruction results through the inverse mapping learned from the other three tasks. It is demonstrated that with mapping memory the same sample can be Associated with any other types of previous task samples. Note that although our model can recall the historical episodes from the current training samples, the generated image still has artifacts, and some extremely distorted locations have blur or noise. This phenomenon is also similar to human cognition, that is to say, the recalled thing is a macroscopic impression, and there may be deviation or lack of memory about the true details of events. This limits the performance of model, making it a gap with MR method where images are completely and mechanically memorized.

4.12 User Study

We conduct a user study with 20 participants to estimate the perception of generated images. We show each participant 60 groups of pictures, each group contains our generated predictions and those of other methods. Participants should point out the most realistic pictures in each group. Table 3 presents the percentage of votes attained by each method in each task. This study indicates that our approach is close to MR but not par with JL. Since JL is the theoretical upper bound of continual learning, it achieves the best visual results and makes participants more satisfied in perception. Compared with MR, which is also a continual learning method, our performance is still very close to it. Despite this, our method has achieved satisfactory results to a certain extent, with a satisfaction rate of approximately 25%. TL does not have the capability for continual learning, its results of all previous tasks can not make participants feel visually satisfied except the most recent task.

	Task1	Task2	Task3	Task4
JL	0.53	0.45	0.38	0.33
TL	0.00	0.00	0.00	0.23
MR	0.18	0.30	0.33	0.20
Assoc-GAN	0.28	0.25	0.28	0.23

Table 3: User Study.

5 Conclusion

In this paper, we explore the catastrophic forgetting problem for generative network and propose a brain-inspired associative learning framework based on the mediation by potentiative heuristics module and depressive feature distillation. We evaluate Assoc-GAN and other generative models on paired image reconstruction task. It demonstrates that Assoc-GAN optimizes the generation performance in the following aspects: 1) generating comparable results to others while not forgetting historical tasks; 2) maintaining the same performance with others while reducing spatial space overhead by up to 94.1%; 3) improving the robustness of model to tasks, the amplitude of fluctuation interference is dropped by up to 88.69%.

Acknowledgements

This work is partially supported by the National Key R&D Program of China (No.2018YFB0105203), NSFC (No.61932014, 61972246), Natural Science Foundation of Shanghai (No.18ZR1418500) and Research Collaboration Grant from NII, Japan.

References

- [1] Michael McCloskey and Neal J Cohen. Catastrophic interference in connectionist networks: The sequential learning problem. In *Psychology of learning and motivation*, volume 24, pages 109–165. Elsevier, 1989.
- [2] Janghyeon Lee, Hyeong Gwon Hong, Donggyu Joo, and Junmo Kim. Continual learning with extended kronecker-factored approximate curvature. In *Proceedings of the IEEE/CVF Conference on Computer Vision and Pattern Recognition*, pages 9001–9010, 2020.
- [3] Davide Abati, Jakub Tomczak, Tijmen Blankevoort, Simone Calderara, Rita Cucchiara, and Babak Ehteshami Bejnordi. Conditional channel gated networks for task-aware continual learning. In *Proceedings of the IEEE/CVF Conference on Computer Vision and Pattern Recognition*, pages 3931–3940, 2020.
- [4] Ashish Gaurav, Sachin Vernekar, Jaeyoung Lee, Vahdat Abdelzad, Krzysztof Czarnecki, and Sean Sedwards. Simple continual learning strategies for safer classifiers. In *SafeAI@ AAI*, pages 96–104, 2020.
- [5] Mohammad Rostami, Soheil Kolouri, Praveen K Pilly, and James McClelland. Generative continual concept learning. In *AAAI*, pages 5545–5552, 2020.
- [6] Rahaf Aljundi, Eugene Belilovsky, Tinne Tuytelaars, Laurent Charlin, Massimo Caccia, Min Lin, and Lucas Page-Caccia. Online continual learning with maximal interfered retrieval. In *Advances in Neural Information Processing Systems*, pages 11849–11860, 2019.
- [7] Ye Xiang, Ying Fu, Pan Ji, and Hua Huang. Incremental learning using conditional adversarial networks. In *Proceedings of the IEEE International Conference on Computer Vision*, pages 6619–6628, 2019.
- [8] Wendy Xin and Jonah R Chan. Myelin plasticity: sculpting circuits in learning and memory. *Nature Reviews Neuroscience*, pages 1–13, 2020.
- [9] Kibok Lee, Kimin Lee, Jinwoo Shin, and Honglak Lee. Overcoming catastrophic forgetting with unlabeled data in the wild. In *Proceedings of the IEEE International Conference on Computer Vision*, pages 312–321, 2019.
- [10] Mengyao Zhai, Lei Chen, Frederick Tung, Jiawei He, Megha Nawhal, and Greg Mori. Lifelong gan: Continual learning for conditional image generation. In *Proceedings of the IEEE International Conference on Computer Vision*, pages 2759–2768, 2019.
- [11] Dongmin Park, Seokil Hong, Bohyung Han, and Kyoung Mu Lee. Continual learning by asymmetric loss approximation with single-side overestimation. In *Proceedings of the IEEE International Conference on Computer Vision*, pages 3335–3344, 2019.
- [12] Richard GM Morris, Eric R Kandel, and Larry R Squire. The neuroscience of learning and memory: cells, neural circuits and behavior, 1988.
- [13] Yadin Dudai. *The neurobiology of memory: concepts, findings, trends*. Oxford University Press, 1989.
- [14] Danke Zhang, Chi Zhang, and Armen Stepanyants. Robust associative learning is sufficient to explain the structural and dynamical properties of local cortical circuits. *Journal of Neuroscience*, 39(35):6888–6904, 2019.
- [15] Marcus E Raichle, Ann Mary MacLeod, Abraham Z Snyder, William J Powers, Debra A Gusnard, and Gordon L Shulman. A default mode of brain function. *Proceedings of the National Academy of Sciences*, 98(2):676–682, 2001.
- [16] Aleksandr Romanovich Luria. *Higher cortical functions in man*. Springer Science & Business Media, 2012.
- [17] Kathleen KA Cho, Thomas J Davidson, Guy Bouvier, Jesse D Marshall, Mark J Schnitzer, and Vikaas S Sohal. Cross-hemispheric gamma synchrony between prefrontal parvalbumin interneurons supports behavioral adaptation during rule shift learning. *Nature Neuroscience*, pages 1–11, 2020.
- [18] Annie Handler, Thomas GW Graham, Raphael Cohn, Ianessa Morantte, Andrew F Siliciano, Jianzhi Zeng, Yulong Li, and Vanessa Ruta. Distinct dopamine receptor pathways underlie the temporal sensitivity of associative learning. *Cell*, 178(1):60–75, 2019.
- [19] Arghya Mukherjee and Pico Caroni. Infralimbic cortex is required for learning alternatives to prelimbic promoted associations through reciprocal connectivity. *Nature communications*, 9(1):1–14, 2018.
- [20] Andrei A Rusu, Neil C Rabinowitz, Guillaume Desjardins, Hubert Soyer, James Kirkpatrick, Koray Kavukcuoglu, Razvan Pascanu, and Raia Hadsell. Progressive neural networks. *arXiv preprint arXiv:1606.04671*, 2016.
- [21] Jaehong Yoon, Eunho Yang, Jeongtae Lee, and Sung Ju Hwang. Lifelong learning with dynamically expandable networks. *arXiv preprint arXiv:1708.01547*, 2017.
- [22] Stephen Marsland, Jonathan Shapiro, and Ulrich Nehmzow. A self-organising network that grows when required. *Neural networks*, 15(8-9):1041–1058, 2002.
- [23] German I Parisi, Jun Tani, Cornelius Weber, and Stefan Wermter. Lifelong learning of human actions with deep neural network self-organization. *Neural Networks*, 96:137–149, 2017.
- [24] Oleksiy Ostapenko, Mihai Puscas, Tassilo Klein, Patrick Jahnichen, and Moin Nabi. Learning to remember: A synaptic plasticity driven framework for continual learning. In *Proceedings of the IEEE Conference on Computer Vision and Pattern Recognition*, pages 11321–11329, 2019.

- [25] Zhizhong Li and Derek Hoiem. Learning without forgetting. *IEEE transactions on pattern analysis and machine intelligence*, 40(12):2935–2947, 2017.
- [26] Geoffrey Hinton, Oriol Vinyals, and Jeff Dean. Distilling the knowledge in a neural network. *arXiv preprint arXiv:1503.02531*, 2015.
- [27] James Kirkpatrick, Razvan Pascanu, Neil Rabinowitz, Joel Veness, Guillaume Desjardins, Andrei A Rusu, Kieran Milan, John Quan, Tiago Ramalho, Agnieszka Grabska-Barwinska, et al. Overcoming catastrophic forgetting in neural networks. *Proceedings of the national academy of sciences*, 114(13):3521–3526, 2017.
- [28] Sang-Woo Lee, Jin-Hwa Kim, Jaehyun Jun, Jung-Woo Ha, and Byoung-Tak Zhang. Overcoming catastrophic forgetting by incremental moment matching. In *Advances in neural information processing systems*, pages 4652–4662, 2017.
- [29] Friedemann Zenke, Ben Poole, and Surya Ganguli. Continual learning through synaptic intelligence. *Proceedings of machine learning research*, 70:3987, 2017.
- [30] Felix Wiewel and Bin Yang. Localizing catastrophic forgetting in neural networks. *arXiv preprint arXiv:1906.02568*, 2019.
- [31] Sylvestre-Alvise Rebuffi, Alexander Kolesnikov, Georg Sperl, and Christoph H Lampert. icarl: Incremental classifier and representation learning. In *Proceedings of the IEEE conference on Computer Vision and Pattern Recognition*, pages 2001–2010, 2017.
- [32] David Lopez-Paz and Marc’Aurelio Ranzato. Gradient episodic memory for continual learning. In *Advances in neural information processing systems*, pages 6467–6476, 2017.
- [33] Chenshen Wu, Luis Herranz, Xialei Liu, Joost van de Weijer, Bogdan Raducanu, et al. Memory replay gans: Learning to generate new categories without forgetting. In *Advances in Neural Information Processing Systems*, pages 5962–5972, 2018.
- [34] Ian Goodfellow, Jean Pouget-Abadie, Mehdi Mirza, Bing Xu, David Warde-Farley, Sherjil Ozair, Aaron Courville, and Yoshua Bengio. Generative adversarial nets. In *Advances in neural information processing systems*, pages 2672–2680, 2014.
- [35] Raymond A Yeh, Chen Chen, Teck Yian Lim, Alexander G Schwing, Mark Hasegawa-Johnson, and Minh N Do. Semantic image inpainting with deep generative models. In *Proceedings of the IEEE conference on computer vision and pattern recognition*, pages 5485–5493, 2017.
- [36] Yijun Li, Sifei Liu, Jimei Yang, and Ming-Hsuan Yang. Generative face completion. In *Proceedings of the IEEE Conference on Computer Vision and Pattern Recognition*, pages 3911–3919, 2017.
- [37] Wenlong Zhang, Yihao Liu, Chao Dong, and Yu Qiao. Ranksrgan: Generative adversarial networks with ranker for image super-resolution. In *Proceedings of the IEEE International Conference on Computer Vision*, pages 3096–3105, 2019.
- [38] Jinshan Pan, Jiangxin Dong, Yang Liu, Jiawei Zhang, Jimmy Ren, Jinhui Tang, Yu Wing Tai, and Ming-Hsuan Yang. Physics-based generative adversarial models for image restoration and beyond. *IEEE Transactions on Pattern Analysis and Machine Intelligence*, 2020.
- [39] Jun-Yan Zhu, Taesung Park, Phillip Isola, and Alexei A Efros. Unpaired image-to-image translation using cycle-consistent adversarial networks. In *Proceedings of the IEEE international conference on computer vision*, pages 2223–2232, 2017.
- [40] Han Shu, Yunhe Wang, Xu Jia, Kai Han, Hanting Chen, Chunjing Xu, Qi Tian, and Chang Xu. Co-evolutionary compression for unpaired image translation. In *Proceedings of the IEEE International Conference on Computer Vision*, pages 3235–3244, 2019.
- [41] Zili Yi, Hao Zhang, Ping Tan, and Minglun Gong. Dualgan: Unsupervised dual learning for image-to-image translation. In *Proceedings of the IEEE international conference on computer vision*, pages 2849–2857, 2017.
- [42] Phillip Isola, Jun-Yan Zhu, Tinghui Zhou, and Alexei A Efros. Image-to-image translation with conditional adversarial networks. In *Proceedings of the IEEE conference on computer vision and pattern recognition*, pages 1125–1134, 2017.
- [43] Ting-Chun Wang, Ming-Yu Liu, Jun-Yan Zhu, Andrew Tao, Jan Kautz, and Bryan Catanzaro. High-resolution image synthesis and semantic manipulation with conditional gans. In *Proceedings of the IEEE conference on computer vision and pattern recognition*, pages 8798–8807, 2018.
- [44] Chaoyue Wang, Chang Xu, Chaohui Wang, and Dacheng Tao. Perceptual adversarial networks for image-to-image transformation. *IEEE Transactions on Image Processing*, 27(8):4066–4079, 2018.
- [45] Olaf Ronneberger, Philipp Fischer, and Thomas Brox. U-net: Convolutional networks for biomedical image segmentation. In *International Conference on Medical image computing and computer-assisted intervention*, pages 234–241. Springer, 2015.
- [46] Christian Ledig, Lucas Theis, Ferenc Huszár, Jose Caballero, Andrew Cunningham, Alejandro Acosta, Andrew Aitken, Alykhan Tejani, Johannes Totz, Zehan Wang, et al. Photo-realistic single image super-resolution using a generative adversarial network. In *Proceedings of the IEEE conference on computer vision and pattern recognition*, pages 4681–4690, 2017.
- [47] Yancheng Bai, Yongqiang Zhang, Mingli Ding, and Bernard Ghanem. Finding tiny faces in the wild with generative adversarial network. In *Proceedings of the IEEE conference on computer vision and pattern recognition*, pages 21–30, 2018.
- [48] Chunjie Luo, Jianfeng Zhan, Xiaohe Xue, Lei Wang, Rui Ren, and Qiang Yang. Cosine normalization: Using cosine similarity instead of dot product in neural networks. In *International Conference on Artificial Neural Networks*, pages 382–391. Springer, 2018.

- [49] Saihui Hou, Xinyu Pan, Chen Change Loy, Zilei Wang, and Dahua Lin. Learning a unified classifier incrementally via rebalancing. In *Proceedings of the IEEE Conference on Computer Vision and Pattern Recognition*, pages 831–839, 2019.
- [50] Yi Gu, Yuting Gao, Jie Li, Chentao Wu, and Weijia Jia. Generative and discriminative learning for distorted image restoration. *arXiv preprint arXiv:2011.05784*, 2020.
- [51] Yaxing Wang, Chenshen Wu, Luis Herranz, Joost van de Weijer, Abel Gonzalez-Garcia, and Bogdan Raducanu. Transferring gans: generating images from limited data. In *Proceedings of the European Conference on Computer Vision (ECCV)*, pages 218–234, 2018.